Supplementary Appendix

A Hereditary Form of Small Intestinal Carcinoid Associated with a Germline Mutation in Inositol Polyphosphate Multikinase

Yoshitatsu Sei, Xilin Zhao, Joanne Forbes, et al.

Table of Contents

I. Online Methods

Clinical Enrollment and Evaluation

Adult patients with small intestinal carcinoid neuroendocrine tumors (SI-NET) were enrolled if they had one blood relative with SI-NET, while asymptomatic adults required at least two blood relatives diagnosed with carcinoid SI-NET. Patients belonging to a family with a known type of familial tumor (Multiple Endocrine Neoplasia types 1 and 2, Neurofibromatosis 1, Von Hippel-Lindau Disease or other familial tumor syndrome) were clinically excluded.

The study was approved by the Institutional Review Board (IRB) of the National Institute of Diabetes, Digestive and Kidney Diseases (NIDDK) and registered with ClinicalTrials.gov (NCT00646022). Previously diagnosed patients and their asymptomatic blood relatives were enrolled after receiving informed written consent. Study subjects were recruited from all over the United States in response either to the listing of the protocol on ClinicalTrials.gov, by reference from a physician, a patient advocacy group, or an affected relative.

All patients were admitted to the NIH Clinical Research Center and underwent evaluation including history, physical exam, biochemical tests (including 24 hour urine 5-hydroxyindoleacetic acid (5-HIAA), whole blood serotonin and histamine, serum chromogranin A, gastrin and pancreatic polypeptide), esophagogastroduodenoscopy (EGD), colonoscopy and ileoscopy, wireless capsule endoscopy, computerized tomography (CT) of the chest, abdomen and pelvis with intravenous contrast and oral Volumen, magnetic resonance imaging (MRI) with contrast of the chest abdomen and pelvis, whole body Octreoscan and 18F-DOPA positron emitted tomography (PET) scan. Asymptomatic family members were similarly re-evaluated every two years with the exception of EGD, colonoscopy, MRI, and Octreoscan. Previously diagnosed and positively screened asymptomatic family members are also

followed at the NIH Clinical Research Center in addition to being followed by their local oncologists.

Octreoscan

Patients received intravenous injection of 220 MBq (6.0 mCi) In-111-pentetreotide. Four hours after injection, patients underwent whole body planar scanning as well as single photon emission computed tomography (SPECT) scans of the head through the pelvis. Scintigraphic and SPECT images were acquired on a dual-head γ-camera (ADAC Laboratories or Siemens Medical Solutions, Malvern, PA) and a triple-head γ-camera (Trionix XLT; Trionix Laboratories, Twinsurg, OH), respectively, equipped with medium-energy general-purpose collimators. A total of 120 sequential 40-s images were obtained. The images were reconstructed with the manufacturer's software using a standard filtered backprojection algorithm. A Hamming filter was used for reconstruction. Repeat SPECT or SPECT/CT was performed at 24 hours, if necessary. Patients were limited to one attenuation CT per body area per study. If patients were on Somatostatin therapy, all scans were performed at least four weeks after discontinuation of therapy.

18F-DOPA PET/CT

Patients were imaged either on a GE Advance PET scanner (PET alone) or Discovery ST PET/CT scanner (GE Healthcare, Wauwatosa, WI) (PET/CT) beginning one-hour after injection with 12 millicuries of 18F-DOPA after pretreatment with Carbidopa, 2 mg/kg up to 200 mg 60 min prior to dosing. Emission scans were acquired for five minutes per bed position with three-minute transmission scans. Patients were scanned from the upper thigh to the midbrain. Lower extremities were not included.

Computerized Axial Tomography (CT) Scans

CT enterography was performed after administration of oral and intravenous contrast. A total of 900 cc

of Volumen (Bracco Diagnostics, Princeton, NJ) at room temperature was administered orally, 450 mL administered from 0-20 minutes and 450 ml at 20-40 minutes followed by 1000 cc of water administered orally from 40 to 60 minutes. Scanning was begun up to 10 minutes after ingestion of water. Scanning was performed on a Siemens Definition (Siemens Healthcare USA, Malvern, PA), Phillips (Phillips Healthcare, Andover, MA), or GE Lightspeed (GE Medical Systems, Waukesha, WI). 130 cc of Isovue-300 (Bracco Diagnostics) was injected intravenously at 5 cc/sec. Arterial phase images were acquired at 30 seconds after the initiation of injection, and venous phase images at 15 seconds after termination of the arterial phase. Axial images were reconstructed at contiguous 1and 2 mm slice thickness, and coronal images at 3 mm thickness.

Magnetic Resonance Imaging (MRI)

MRI scans were obtained at 1.5 or 3.0 Tesla using the Philips Achieva MRI. (Philips Healthcare, Netherlands). For MRI of the chest, T2 axial with and without fat suppression, T1 fat suppression pre- and post- Magnevist injection (Bayer Health Care Pharmaceuticals, Whippany, NJ), delayed axial and coronal post-contrast images were obtained. For MRI of the abdomen, T2 with and without fat suppression, in and out of phase imaging, and dynamic pre- and post-contrast THRIVE imaging were obtained. For MRI of the pelvis, T1 axial pre- and post-Magnevist injection (Bayer Health Care Pharmaceuticals), in and out of phase imaging, and delayed axial and coronal images were obtained. Magnevist was injected intravenously at a concentration of (0.1mmol/kg) unless contraindicated by renal insufficiency.

Serotonin, Chromogranin A, Synaptophysin and Ki-67 Immunohistochemistry

Immunohistochemistry was performed on all tumor samples using an automated immunostainer (Ventana Medical Systems, Inc., Tucson, AZ), according to the company's protocols, with slight modifications. After deparaffinization and rehydration, heat-induced antigen retrieval was performed for all antibodies with the exception of serotonin. Slides were placed in a microwave pressure cooker (TenderCooker, Nordicware, Minneapolis, MN) in 0.01 mol/L citrate buffer, pH 6.0, containing 0.1% Tween 20, and heated in a microwave oven at maximum power for 20 minutes. Thereafter, sections were washed in Tris-buffered saline (pH 7.6) containing 5% fetal calf serum (Life Technologies, Grand Island, NY). The slides were then transferred to the automated stainer, and primary antibody incubation (32 minutes) and detection was carried out using the Ventana ultraView DAB Detection Kit. Positive controls were used to confirm the adequacy of the staining for each antibody. Antibodies were used at the following dilutions: chromogranin A, (clone LK2H10), 1:200, (Neomarkers, Freemont, CA); Ki-67 (MIB-1), 1:200, and serotonin (5HT-H209), 1:200, (Dako Corp, Carpinteria, CA); synaptophysin 1:100, Invitrogen (Life Technologies, Grand island, NY).

Blood Samples

Peripheral blood samples were obtained from subjects. Isolation of lymphocytes and EBV-transformation were conducted at the Johns Hopkins Institute of Genetic Medicine in the Genetic Resources Core Facility (Baltimore, MD) on four affected patients and their age-matched spouses as well as four family members without the *IPMK* mutation.

Cell Cultures

The EBV-transformed B lymphoblasts were grown in RPMI-1640 medium (Gibco, Grand Island, NY) containing 10% heat-inactivated fetal bovine serum (FBS) (Gibco), L-glutamine (2 mmol/L), 100 mg/mL streptomycin and 100 units/mL penicillin (Gibco) in an incubator (95% air/5% CO_2 at 37°C). HEK293 cells were purchased from the American Tissue Culture Collection (ATCC, Manassas, VA) and cultured in DMEM (Gibco) containing 10% FBS, L-glutamine (2 mmol/L), 100 mg/mL streptomycin and 100 units/mL penicillin in an incubator (95% air/5% CO_2 at 37°C).

Germline Genotyping

Single nucleotide polymorphism (SNP) genotyping was performed on samples from pedigrees 1, 7, and 9 using the GoldenGate Linkage V SNP-based linkage panels GS0007351-OPA and GS0007352-OPA consisting of 3031 SNPS. Genomic DNA, extracted from either whole blood, saliva or normal tissue in FFPE tissue blocks was amplified and processed on an automated Illumina Tecan workstation according to the manufactures protocol, imaged on a Universal Bead Chip using the Illumina iScan Reader and analyzed using Illumina Genome Studio software (Illumina, Inc., San Diego, CA).

Genotypes were called on 2571 autosomal SNPs. Markers with high missing genotype call rates (> 10%) were dropped. Due to batch effects, SNPs with called genotypes were non-uniformly distributed across the genome and this affected subsequent choice of markers for fine mapping. Sequence analysis was done in parallel with genetic linkage analysis and also had an effect on selection of markers for fine mapping. Genotypes were checked against family relationships using PREST[1] and SIB-PAIR (http://genepi.qimr.edu.au/staff/davidD/Sib-pair/Documents/sib-pair.html) to detect genotype errors, reporting errors, and sample swaps in the lab. SNPs with excessive Mendelian errors (more than 2) were dropped. For SNPs that exhibited only a single Mendelian error in the dataset, we dropped that SNP's

genotypes for the family in question. We further used PLINK[2] to prune out non-independent SNPs to achieve a set with bounded inter-marker linkage disequilibrium ($D' < 0.8$ and $R^2 \leq 0.1$) among them. The remaining 1230 SNP genotypes were included in the initial linkage analysis. Based on the results of this SNP-only linkage analysis, fine mapping was conducted using 15 microsatellite markers under a linkage peak with suggestive evidence of linkage, in order to obtain denser, more uniform coverage of this region with more information content. Both microsatellite genotypes and SNP genotypes were used in our final linkage analysis. SIB-PAIR was used to detect Mendelian inconsistencies, to impute unambiguous genotypes for non-genotyped parents and to estimate allele frequencies for each marker using founders only. Genetic distances for SNP and microsatellite markers were based on the Rutgers combined linkage-physical mapv2(build 36)[1]and Rutgers Map Interpolator (http://compgen.rutgers.edu/mapinterpolator) was used to estimate genetic distance for markers not on the map.

Microsatellite genotyping: Microsatellites D10s595 , D10s1214, D10s1793, D10s196, D10s220, D10s539, D10s1790, D10s1226, D10s1756, D10s464, D10s589, D10s1652, D10s1672, D10s1730 and D10s1717 were amplified using the following PCR conditions: 12 min denaturation at 95°C; 10 cycles of 94°C for 45 sec, 55°C for 1 min, and 72°C for 1 min; 20 cycles of 89°C for 1 min, 55°C for 1 min, and 72°C for 1 min; 10 min final extension at 72°C.

Genotype calling: Fragment separation was achieved by capillary electrophoresis on a Genetic Analyzer 3130 using 36cm capillary array and POP-7 polymer. The ROX400 size standard (Applied Biosystems, Foster City, CA) was run as an internal size-standard. Allele size was calculated using the local Southern algorithm available in the GENESCAN software program (Applied Biosystems). Allele calling and binning was done using the GENOTYPER software. (GeneScan and Genotyper are no longer

commercially available and have been combined in GeneMapper, Applied Biosystems). All genotyping was done including a CEPH control individual #134702 (Applied Biosystems) for quality control purposes.

Tumor SNP Genotyping

The primary scan for matching patient buffy coat and tumor DNA samples was performed at the NCI Core Genotyping Facility using Human 660W-Quad Infinium BeadChips (Illumina Inc., San Diego, CA) via the Infinium Assay following manufacturer recommendations. All Illumina genotyping samples exceeded a SNP call rate >99%, and a LogRdev value <0.2. The data were analyzed using an Allele specific Copy Number Analysis of Tumors (ASCAT) algorithm[2]. Estimates of tumor ploidy as a percentage of non-aberrant cell admixture were computed using log ratio values and B-allele frequencies (BAF) were estimated from the SNP array data. The log ratio threshold for high copy gain (2 or more copies) was set at 2. The Max Contiguous Probe Spacing was set at 1000 Kbp. The Homozygous Value Threshold was set to 0.8. The Breakpoint Significance Threshold for segmentation was set at 1.0E-5 also requiring a minimum of 3 probes per segment. Gamma (modeling the spread of the data) was set at 0.55. All tumor samples were matched with corresponding germline samples using matched pair-analysis computation.

Illumina output files were analyzed using Nexus Copy Number version 6 (BioDiscovery, Hawthorne, CA), which applies a "Rank Segmentation" algorithm based on the circular binary segmentation (CBS) approach[3]. "SNPRank Segmentation", an extended algorithm in which BAF values are also included in the segmentation process, generated both copy-number and allelic event calls. The software default calling parameters were applied for analysis using BAF and Log R ratio (LRR) for determination of Copy Number Variation (CNV).

Genetic Linkage Analysis

Genetic linkage analysis of pedigrees 1, 7, and 9 was done. In this paper, we focus on pedigree 9 because it is the only one that can achieve genome-wide linkage significance by itself and there was strong evidence that pedigrees 1 and 7 do not share the linkage region with pedigree 9 (Fig. S3). For linkage analysis of pedigree 9, only individuals with a diagnosis of carcinoid tumor on the basis of surgical pathology (n = 8), clinical history (n =1), abnormal CT imaging (n=1) or elevated 24 hour urinary 5-hydroxyindoleacetic acid level (n =1) were coded as affected (2). Unrelated normal spouses as well as a few "super-normal" family members (negative biochemical and imaging evaluation at the NIH CRC as described above and over 64 years old (n = 2) or age 53 and negative surgical exploration at the NIH CRC (n = 1)) were coded unaffected (1) in the analysis. Unaffected individuals without any offspring and without genotype data were removed from the pedigrees for the analysis and all remaining individuals were coded as unknown (0).

Model-based linkage analysis was performed assuming a biallelic major locus (the disease-predisposing allele is denoted as D and the other allele as d). One liability class was used to model a dominant model with complete penetrance of the D allele and no phenocopies. The frequency of the D allele was set to 0.05. Sensitivity analyses were performed for markers on chromosome 10 where significant linkage was identified. Several different reduced penetrance models were utilized bounded by the full penetrance model given above and a dominant model with reduced penetrance (penetrance specified to be 0.5 and 0 for genotypes DD/Dd and dd). Furthermore, model-free linkage analysis using the NPL_ALL option in Simwalk2[54] was done (Fig. S2), resulting in a multipoint non-parametric linkage p-value less than 0.0001.

Fine-mapping in the region of suggestive linkage on chromosome 10 was performed using 15

microsatellite markers that passed quality control procedures. These markers were selected for fine-mapping genotyping because they were known to be highly heterozygous and approximately uniformly spaced across the linkage region.

To test if the identified mutation is able to explain fully the linkage signal, the putative causal mutation under the linkage peak, which had been discovered in the WES analysis, was genotyped in all family members and combined with the SNP and microsatellite marker genotypes in a multi-marker parametric linkage analysis. Additionally, single-marker linkage analyses were performed for the putative causal mutation and each SNP and microsatellite marker on chromosome 10 separately using disease allele frequencies of 0.05 and 0.005 (Fig. 2c).

Simwalk2[4] was used for both model-based and model-free multi-marker linkage analyses as well as for haplotype analysis for markers at the linkage signal. Single-marker LOD scores were computed with FASTLINK[5, 6].

Power calculations were done with the simulation software FastSLINK[7, 8] using one or more markers with heterozygosity of 0.8 (five equi-frequent alleles) or a SNP with two equi-frequent alleles. The power calculations assumed full penetrance since the best LOD scores in the observed data were achieved with a full penetrance dominant model. The purpose of the power calculations was to compare the observed LOD scores with LOD scores that the simulations suggest are best possible, conditional on the pedigree structure and observed phenotypes.

Whole Exome Sequencing (WES) and Variant Analysis

A genomic library was prepared using peripheral blood mononuclear cell DNA from five (initially four, one added later for confirmation) affected members of family 9 and one unaffected member

using the Paired-End DNA Sample Prep Kit V1 (Illumina, Inc., San Diego, CA). The library was exome enriched (101 bp paired-end read library hydridized to Agilent SureSelect Human All Exon capture kit V4 (37 Mb) for 9:III-2 and 9:III-12 and V5 (50 Mb) for 9:II-3, 9:III-3, 9:III-11 and 9:III-22 (Fig. 2A and S1 and Table S1). WES was performed with an Illumina Genome Analyzer II initially and subsequently with the HiSeq 2000. The sequence runs were 101 bp paired-end reads that were aligned to human reference genome (NCBI build 36) using SRPRISM (unpublished, available at ftp://ftp.ncbi.nlm.nih.gov/pub/agarwala/srprism/). Coverage for the targeted exome was >100X with 90-96% of reads uniquely mapped, 95% of exon regions with >10x coverage and 99% of targeted exons mapped with a *phred*-like consensus quality ≥ 20. In the initial analysis using the Sequence Variant Analyzer (SVA)[9] pipeline, only heterozygous single nucleotide variants (missense and nonsense), splice site mutations, and small coding indels not reported in the available dbSNP version (131 in initial analysis, 135 in confirmatory analysis) and shared by all sequenced affected individuals but not shared by the unaffected individual were considered. In the confirmatory analysis of the five affected individuals, NextGENe software (SoftGenetics, College Station, PA) was used to consider small coding indels and heterozygous single nucleotide variants (missense and nonsense), and splice site mutations in dbSNP135 and dbNSFP 2.0 (includes 1000 Genomes and ESP6500 data of the National Heart, Lung, and Blood Institute GO Exome Sequencing Project (http://evs.gs.washington.edu/EVS) with a minor allele frequency (MAF) ≤ 0.001).

Mutation Validation

Sanger sequencing of PCR amplicons of consensus coding sequence cDNA derived from peripheral blood mononuclear cell RNA was used to verify the candidate gene variants in the linkage interval and shared variants outside the linkage interval suspected from WES of family #9 (Fig. 2) and also to screen

at least one affected individual from each of the other families (Fig. S1) in whom indels, synonymous, non-synonymous and nonsense variants were considered.

Laser capture micro-dissection

Laser capture micro-dissection of tumor tissue was performed using an Arcturus Ventris unit (Life Technologies, Carlsbad, CA, USA). Ten μm tumor sections placed onto polyethylene napthalate (PEN) membrane slides were stained with hematoxylin and eosin. Morphologically identified areas of tumor cells were cut with UV laser and captured using a near-infrared laser pulse for transfer onto a cap (Capsure™ Macro LCM Caps, Life Technologies, Frederick, MD). DNA was extracted from the cells adherent to the cap by overnight proteinase K digestion at 56°C and subsequent incubation at 90°C for 1h. Extracted DNA was purified using the QIAamp DNA micro kit (Qiagen, Valencia, CA) according to the manufacturer's instructions.

Detection of IPMK Protein

B lymphoblastoid cells were incubated in lysis buffer containing 50 mM Tris-HCl (pH 7.4), 100 mM NaCl, 2 mM EDTA, 1 mM Vanadate and complete ultra protease inhibitor cocktail (Roche Applied Science, Germany) for 20 min at 4°C. Following centrifugation at 14,000xg for 15 min, the supernatants were collected. The protein samples (400 mg) were subjected to immunoprecipitation for IPMK using the Co-IP kit (Pierce Chemical, Rockford, IL) according to manufacturer's recommendations. The protein samples were incubated overnight with a resin coupled with an antibody to IPMK (aa301-aa337)(T3631, Epitomics, Burlingame, CA). The eluted or input protein samples were separated using NuPAGE 10% Bis-Tris gel (Invitrogen, Carlsbad, CA). After separation, the proteins were transferred to polyvinylidene difluoride membrane (Millipore Corp, Bedford, MA). The membrane was first

incubated with SuperBlock blocking buffer (Thermo Scientific, Rockford, IL) and then probed with an antibody to IPMK (aa26-aa265)(S0838) (Epitomics) or an antibody to β-tubulin (2128) (Cell Signaling Technology, Danvers, MA). To detect the primary antibodies, horseradish peroxidase- conjugated anti-rabbit IgG antibody (1:200,000) (Thermo Scientific, Rockford, IL) was used. Chemiluminescence detection was performed using SuperSignal West Dura or Fempt signal substrate (Thermo Scientific). The protein bands within the linear range of the standard curve were imaged and the relative optical density of each band was measured and analyzed using Image J[10]software (NIH, Bethesda, MD).

Construction of GFP-tagged IPMK (with and without 4 bp deletion) Expression Vectors

A construct in which the human *IPMK* gene (NM 152230.2) was cloned into C-terminal MYC/DDK-tagged pCMV entry was purchased from Origene (Rockville, MD) and subcloned into pCMV6-AN-tGFP (Origene) at Sgf1 site. A similar construct carrying a 4 bp deletion in *IPMK* (cDNA bp 993-996, referred to as mutant *IPMK*) was also created by *in situ* mutatgenesis.

Overexpression of WT and Mutant IPMK

C-terminal MYC/DDK-tagged-IPMK (Origene), tGFP-tagged WT-IPMK and mutant IPMK were transfected using of Lipofectamine 2000 (Invitrogen) in six-well plates (Corning Incorporated Life Sciences, Lowell, MA), 96-well plates (Corning), or 8-well m-slides (ibidi, LLC, Verona, WI) according to each manufacturer's recommendation. The HEK-293 cells were transfected at 70% confluency. Transfection efficiencies ranged between 70-90%, assessed by fluorescence microscopy. Transfection efficiency correlated with cell lysate IPMK immunoblotting intensity.

Cell Survival/Proliferation Assay

B lymphoblastoid cells ($2x10^4$ per well) were cultured in 96-well plates. Cells were treated with or

without 0.25-1mM staurosporine (Sigma, St. Louis, MO) or 12.5-50 mM cisplatin (Sigma) in 5% CO_2 incubator at 37°C. After overnight or 24 hrs of culturing, the cell viability was measured by a colorimetric assay using WST-1 (Clontech Laboratories, Mountain View, CA).

RNA Extraction and Semi-Quantitative RT-PCR

Total RNA was extracted from B lymphoblastoid cells using the Nucleospin RNA XS (Macherey-Nagel GmbH & Co. KG, Germany) and reverse transcription performed to generate the first strand of cDNA using Maxima first strand cDNA synthesis kit (Fermentas, Glen Burnie, MD). Synthesized cDNA was then amplified by PCR using Platinum PCR Supermix (Invitrogen) and a primer set that were designed to amplify IPMK selectively over pseudogenes. The sequences of primers for IPMK were 5'-ATTCAGCAACAGGTCAGCAA-3' (sense) and 5'-AATCTATCATTCGCACTTCT -3' (antisense).

Semi-quantitative RT-PCR was attempted by comparison with expression of a housekeeping gene, b-actin. The sequences of primers for b-actin were 5'-AAGAGAGGCATCCTCACCCT-3' (sense) and 5'-TGCTGATCCACATCTGCTGGA-3' (antisense). The amplification was performed with no-RT controls using the optimal number of cycles to ensure that the amplification was completed within the exponential range. The expected size of RT-PCR products for IPMK and b-actin were 676 bp (804..1479 bp of NM_152230.4) and 895 bp (263..1159 bp of NM_001101.3), respectively. The signal ratio of IPMK to ®-actin was determined on the basis of the ratio of the intensity of the PCR product compared with the corresponding ®-actin band. The PCR products were imaged and the relative optical density of each band was measured and analyzed using NIH Image J[10] software.

RNA Extraction and Quantitative RT-PCR

Total RNA was extracted from 0.5 x10^6 B lymphoblastoid cells or tumor using the Nucleospin RNA XS (Macherey-Nagel GmbH & Co. KG, Germany) and reverse transcribed using the High-Capacity cDNA Reverse Transcription kit (Applied Biosystem, San Jose, CA) to generate the first strand of cDNA under the following conditions: 5 minutes at 25°C, 60 minutes 37°C, and 5 minutes at 95°C. The qPCR reaction was performed using an Applied Biosystems Step One System with a 20 uL reaction volume made of 2X Master Mix with 1 uL target probe for hIPMK (Hs00852670_g1)(common to both Mut- and WT-IPMK, Applied Biosystems, San Jose, CA), 20X Assay Mix, 10X amplified cDNA sample, and water. The ABI pre-set cycling conditions were 10 minutes at 95°C, and then 40 cycles at 95°C for 15 sec, 60°C for 30 sec and 72°C for 1 min. Detection of amplification relied on monitoring a reporter dye (6-FAM). Human β-actin was used as the housekeeping gene to normalize for RNA sample input variability. Sample reactions without RT were used to confirm the absence of contaminating genomic DNA. Gene expression was analyzed using the comparative CT method (ABI User Bulletin #2). Gene expression was normalized as described in the previous subsection. Statistical significance was determined by a two-tailed paired Student's t-test between the ΔC_T values for IPMK from cells or tumor with homozygous WT-IPMK vs. heterozygous Mut-/WT-IPMK.

Sanger Sequencing of *IPMK*

DNA was extracted from 400 μl of patient and de-identified NIH blood bank research donor whole blood using the Maxwell 16 Blood DNA Purification kit (Promega, Madison, WI) and cDNA was prepared from either the same whole blood mononuclear cells or EBV transformed lymphoblasts as described earlier. *IPMK* exons 1-5 coding sequences were PCR amplified from cDNA using AmpliTaq Gold 360 DNA Polymerase with the primers, 5'-AGCCTGAGCGACCCTCG-3' (forward) and 5'-AGGACAACTGTCAGACACAGAAGTAC-3' (reverse). This primer pair covers positions 233..1188 of

the cDNA. Exon 6 coding sequence was amplified from genomic DNA using AmpliTaq Gold 360 DNA Polymerase and the *IPMK* gene selective primers (vs. psuedogenes on chromosomes 13 and 19) 5'-GCCTGGAATCCTGTTTCTTAAG-3' (forward) and 5'-GCAGTCAATATCTGCACCTTTAATGC-3'(reverse). Sanger DNA cycle sequencing was performed with the reverse sequencing primers 5'-GCTGTTGCTGCCAGTAT-3' for the exon 1-5 amplicon (the resulting PCR product extends to position 1012 and covers part of exon 6) and 5'-GCCAATCATAATGAAGAG-3' for the entire exon 6 amplicon.

Confocal Microscopic Image Analysis

Twenty-four hour post-transfection, the HEK293 cells in 8-well m-slides (ibidi) were fixed in 4% paraformaldehyde in phosphate-buffered saline (PBS; pH 7.4) for 30 min. After fixation, the nuclei were stained with 4',6-diamidino-2-phenylindole (DAPI, Sigma) in PBS for 10 min. After washing in PBS, the chambers were filled with PBS and examined using a Zeiss LSM510 Meta confocal microscope (Carl Zeiss, Thornwood, NY).

IPMK Immunohistochemistry

Four micron sections of formalin fixed paraffin-embedded tumor tissue sections were deparaffinized in xylene and dehydrated in graded ethanol. To retrieve the antigen, sections were treated with sodium citrate buffer (10 mM sodium citrate, pH 6.0, with Tween 20) at 95°C for 30 min. Immunohistochemistry (IHC) staining of the tumor tissue sections was then performed using Histostain-Plus 3rd Generation IHC Detection kit (Invitrogen, Cat#. 85-9673) according to the manufacturer's instruction. Following inactivation of the endogenous peroxidase activity and incubation with a protein-blocking solution, slides were incubated with anti-IPMK rabbit polyclonal antibody (Sigma, # HPA037837, 1:25 dilutions) for 1 hour at room temperature in a humidity chamber. Negative

controls were prepared by incubating with rabbit serum. After three washes with PBS, the tissue sections were incubated with a universal secondary biotinylated antibody for 10 min and washed with PBS three times. The sections were then incubated with streptavidin–peroxidase conjugate for 10 min at room temperature. After three washes with PBS, the chromogenic reaction was carried out by incubation of the sections with diaminobenzidine (DAB). Tissue sections were counterstained with hematoxylin (Invtrogen), mounted and examined by light microscopy.

RNA In Situ Hybridization

Expression of mRNA on the formalin fixed paraffin-embedded human tissue sections (either 5 μM carcinoid tumor sections or normal organ tissue arrays, consisting of 30 organs in duplicate (Cat# IMH-373, IMGENEX, San Diego, CA)) were examined by *in situ* hybridization system (QuantiGene View RNA ISH tissue assay) with probes specific to either h*IPMK* (VA1-12881-01, type1, Affymetrix, Santa Clara, CA) or hTPH1 (VA6-12882-01, type 6, Affymetrix, Santa Clara, CA) using Quantigene ViewRNA ISH tissue assay system (Affymetrix) according to the manufacturer's instruction. The chromogens (Fast red and Fast blue) used to label RNA were examined using both bright field and fluorescence microscopy. For the former, tissue sections were examined by light microscopy after counterstain with Gill's hematoxylin. For the latter, the sections were stained with DAPI and examined with optimal excitation/emission settings using Zeiss LSM510 Meta confocal microscope (Carl Zeiss).

Ipmk Expression Along the Small Intestine

C57BL/6 mice were euthanized with CO_2, perfused with cold PBS followed by 4% paraformaldehyde (PFA) in PBS via cardiac perfusion. The resected small intestine was fixed in 4% PFA, impregnated with 30% glucose, divided into 3 equal segments that were embedded in paraffin and cut into 5 ∝m sections

along the longitudinal axis. *In situ* hybridization was performed using Type 6 (fast blue labelling) *mIpmk* probe (catalogue #VB6-14930) and the QuantiGene ViewRNA ISH Tissue Assay Kit (Affymetrix). The slide images were scanned at 40X magnification using an Aperio Scanscope (Aperio, Vista, CA) and analyzed using Aperio Image Analysis positive pixel count algorithm to quantify villus mucosal expression of m*Ipmk* from the average of 5 fields sampled every 1.5 cm along the length of the small intestine.

Subcellular Localization of IPMK in HEK293 Cells. The subcellular localization of IPMK was examined using a human embryonic kidney cell line, HEK293. To determine subcellular localization of the protein, HEK293 cells were transfected transiently with carboxy-terminal tGFP-tagged full-length IPMK wild type or IPMK with 4 bp deletion (mutant IPMK). After 24 hrs, the cells were fixed in 4% paraformaldehyde, stained with DAPI and examined using a confocal microscope, Zeiss LSM 510. The nuclear versus cytoplasmic localization was analyzed from three independent transfections by two-way ANOVA and Bonferroni post hoc test.

Cisplatin-induced Increases in BAX, p21 and PUMA Transcripts

Patients' lymphoblasts were plated in 6-well plates ($1x10^6$ in 5ml media per well) and incubated with or without 50 μM cisplatin in 5% CO_2 incubator at 37°C. After 24 hours of the incubation, total RNA was extracted and subjected to qRT-PCR analysis as described above using specific TaqMan probes for PUMA (BCL2 binding component 3, Hs00248075_m1), BAX (BCL2-associated X protein, Hs00180269_m1) and p21 (cyclin-dependent kinase inhibitor 1A, Hs00355782_m1). Following normalization to β-actin (dCT), cisplatin induced changes in transcript levels relative to baseline (ddCT) were obtained. Treatment-induced fold change in transcript level was then calculated as described above in the subsection entitled "RNA Extraction and Semi-Quantitative RT-PCR".

Simultaneous Detection of DNA Damage and Apoptosis

Cisplatin-induced DNA damage and apoptosis were assessed on affected patient's (*IPMK* mutant) and control (WT *IPMK*) lymphoblasts by flow cytometric measurements of gH2AX and cleaved poly (ADP-ribose) polymerase (PARP). B lymphoblasts were plated in 6-well plates at density of $1x10^6$ cells per well in 5 ml media and incubated with or without 50 mM cisplatin in 5% CO_2 incubator at 37° C for 16 hrs. Cells were fixed with Phosflow Fix Buffer I (BD Bioscience) for 20 min on ice and washed with Phosflow Perm/Wash Buffer I (BD Bioscience). The cells permeabilized in Phosflow Perm/Wash Buffer I were then stained with Alexa488-conjugated anti-H2AX pS139 antibody (Biolegend 613406) and PE-conjugated antibody to the 89 kDa fragment of cleaved PARP (BD Pharmingen, clone F21-852). After washing twice with Phosflow Perm/Wash Buffer I, cells were analyzed using BD LSRII (BD Bioscience). BD FACSDiva software (BD Bioscience) was used to acquire and quantify the fluorescence signal intensities.

Caspase-3 Assay

Activation of caspase-3 was assessed by flow cytometric measurements of cleaved caspase-3. HEK293 cells were plated in 6-well plates at density of $8x10^5$ cells per well, and transfected with the indicated plasmid constructs 24 hrs after the culture was initiated. After 24 hrs of transfection, cells were treated with staurosporene (ST) (0, 0.5 and 1 mM) for 2 hrs, fixed with Phosflow Fix Buffer I (BD Bioscience) for 10 min at 37°C and washed with Phosflow Perm/Wash Buffer I (BD Bioscience). The cells permeabilized in Phosflow Perm/Wash Buffer I were then stained with fluorescein isothiocyanate-(FITC)-conjugated anti-cleaved caspase-3 antibody (#51-68654X, BD Biosciences) for 1 hr at room

temperature. After washing twice with Phosflow Perm/Wash Buffer I, cells were analyzed using FACScan (BD Bioscience). CellQuest software (BD Bioscience) was used to acquire and quantify the fluorescence signal intensities.

Propidium Iodine (PI) Exclusion Assay

HEK293 cell viability was also determined by PI exclusion assay using flow cytometry. Cells were plated in 24-well plates at density of $2x10^5$ cells per well, and transfected with the constructs 24 hrs after the culture was initiated. Twenty-four hours following transfection, cells were treated with ST (0, 0.5 and 1 mM) for 4 hrs, washed once with PBS and incubated with PI in PBS containing 2%FBS for 15 min on ice. The cells were then analyzed to determine proportion of PI exclusion using FACScan (BD Bioscience).

Statistical Analysis

Statistical analysis other than the genetic linkage analysis was performed using Prism version 5.0a (GraphPad Software Inc., La Jolla, CA) or Statview software version 5.01 (*SAS* institute Inc., Gary, NC). Between group comparison of disease stage for cases diagnosed before the study began versus cases diagnosed by the screening that is part of this study used the Chi Square test. Between group comparisons for *in vitro* data were performed using an unpaired *t* test. The disease/genotype- and *in vitro* treatment-interactions were assessed by two-way ANOVA. Data were expressed as mean$\pm$SEM.

II. Supplementary Discussion

Here we add to the discussion in the main document.

IPMK Function:

In addition to its non-enzymatic activity, IPMK has soluble inositol phosphate and lipid kinase activity that have opposing effects on AKT signaling. IPMK increases AKT signaling and proliferation via its lipid kinase activity[11]. However, inositol phosphate kinase activity also increases inositol phosphates and precursors of pyrophosphates that antagonize AKT signaling and promote apoptosis[12-15]. IPMK recruitment to the cell membrane and subsequent inositol phosphate kinase dependent production of IP5 mediates Wnt/b-catenin signaling and activation of Lef/Tcf–sensitive gene transcription via activation of casein kinase 2 (CK2) and inhibition of glycogen synthase kinase 3b (GSK3b)[16, 17]. A recent study shows that nuclear IPMK PI3K activity regulates mRNA export of selective transcripts including *RAD51* and other transcripts necessary during DNA repair in response to genotoxic stress[18]. All of these studies have been performed *in vitro* in a variety of cultured cells and it is unclear to what extent the balance of these growth and apoptotic actions of IPMK apply to the particular 4 bp deletion and subsequent truncation of IPMK that leads to the development of carcinoid tumors in family 9.

III. Supplementary Figures

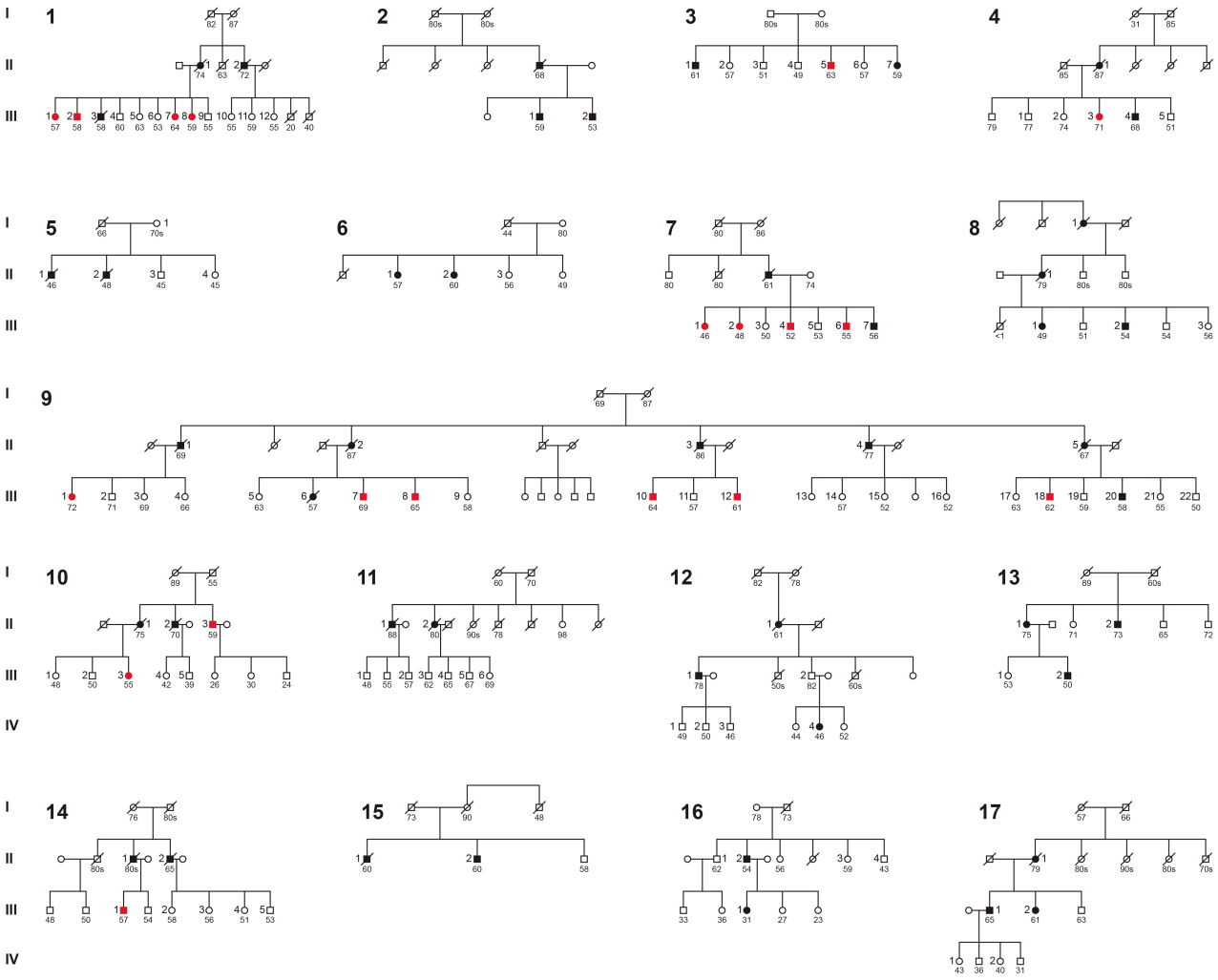

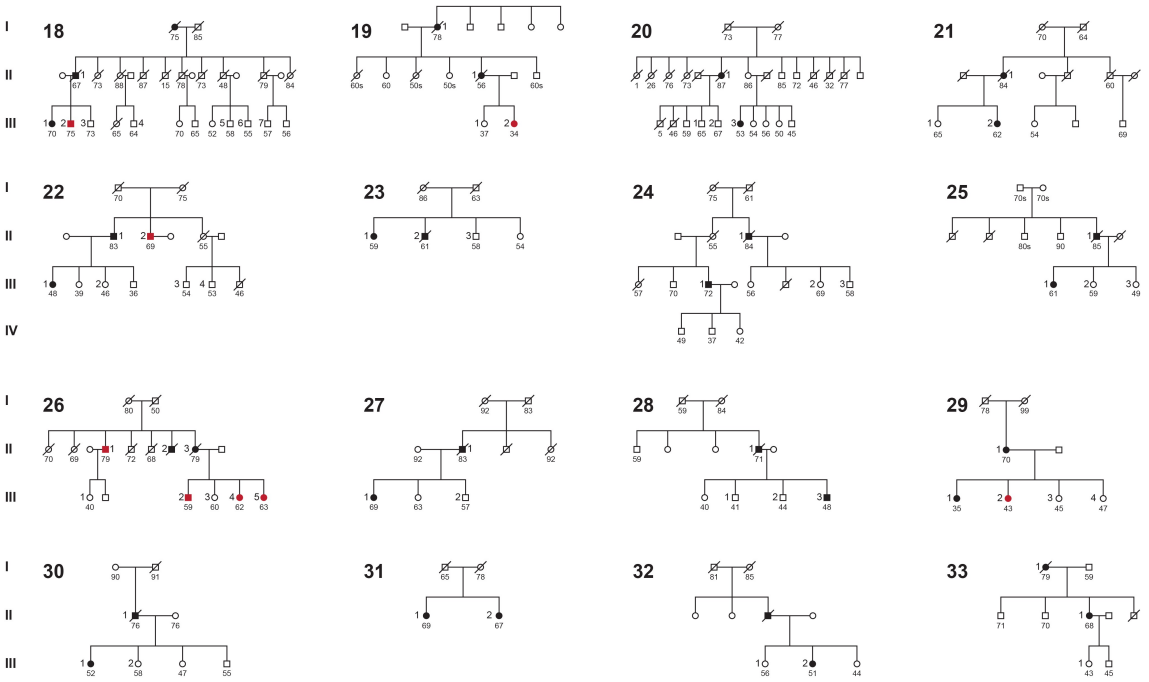

Supplementary Figure S1 Pedigrees of 33 Families with at Least Two First Degree Relatives with Carcinoid Tumor. Affected males (squares) and females (circles) appear as filled symbols. Red filled symbols represent asymptomatic family members with occult tumor diagnosed in this study. Slashes indicate deceased family members. Large bold Arabic numerals identify individual families. Roman numerals to the left indicate family generations. Small Arabic numerals beside a symbol identify individuals included in Table 1 and Supplementary Tables 1 and 2. Small Arabic numerals below a symbol indicate the age of the subject, if alive, or at the time of death. The inheritance pattern is autosomal dominant with incomplete penetrance.

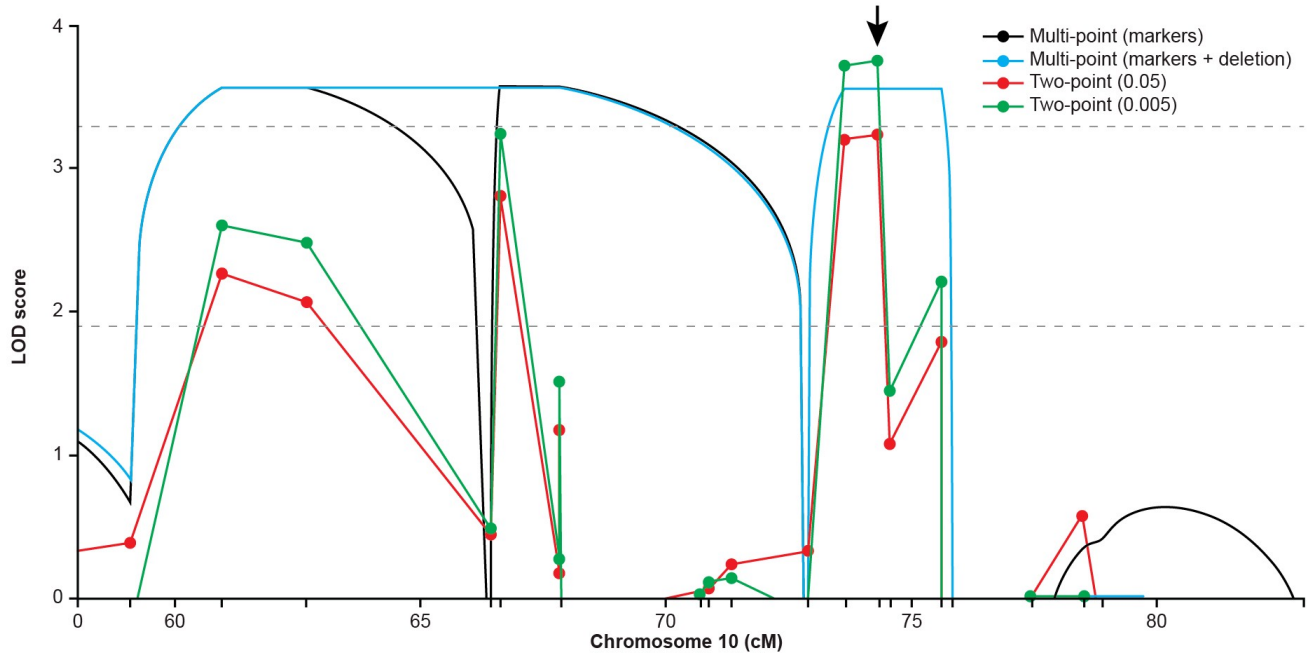

Supplementary Figure S2 Multi-marker and Single-marker Linkage Analysis for Family 9 and Markers in Linkage Region on Chromosome 10. Multi-marker LOD scores for analyses using marker genotypes only and for analyses using the markers plus the *IPMK* deletion genotypes (assuming disease risk allele frequency of 0.05, complete penetrance of the disease allele and zero penetrance in normal homozygotes) are shown as blue and cyan lines. These LOD scores (recombination fraction = 0) were almost identical in the region near the deletion. Red and orange dots denote single-marker two-point LOD scores for analyses assuming the same penetrance and disease allele frequencies of 0.05 and 0.005, respectively. LOD score thresholds for suggestive (LOD ≥1.9) and genome-wide significance (LOD ≥ 3.3)[19] are shown as dotted lines. The star indicates the location of the *IPMK* deletion allele, which has the highest two-point LOD score of all genotyped markers in the region for both assumed disease allele frequencies.

A

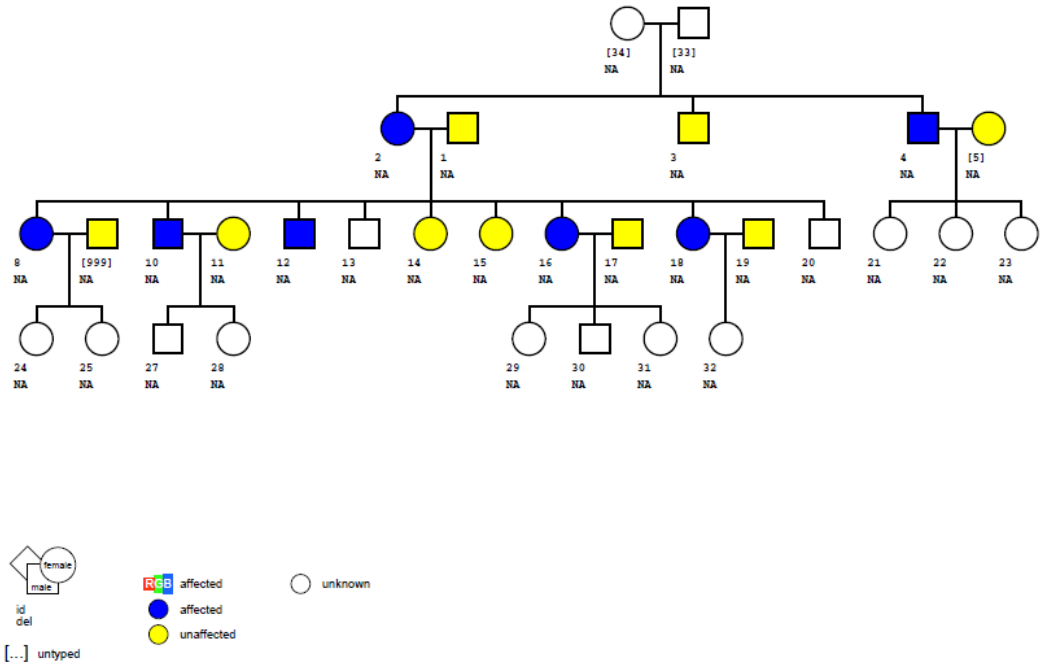
[34]
NA
[33]
NA
2
NA
1
NA
3
NA
4
NA
[5]
NA
8
NA
[999]
NA
10
NA
11
NA
12
NA
13
NA
14
NA
15
NA
16
NA
17
NA
18
NA
19
NA
20
NA
21
NA
22
NA
23
NA
24
NA
25
NA
27
NA
28
NA
29
NA
30
NA
31
NA
32
NA
female
male
id
del
[...] untyped
affected
affected
unaffected
unknown

B

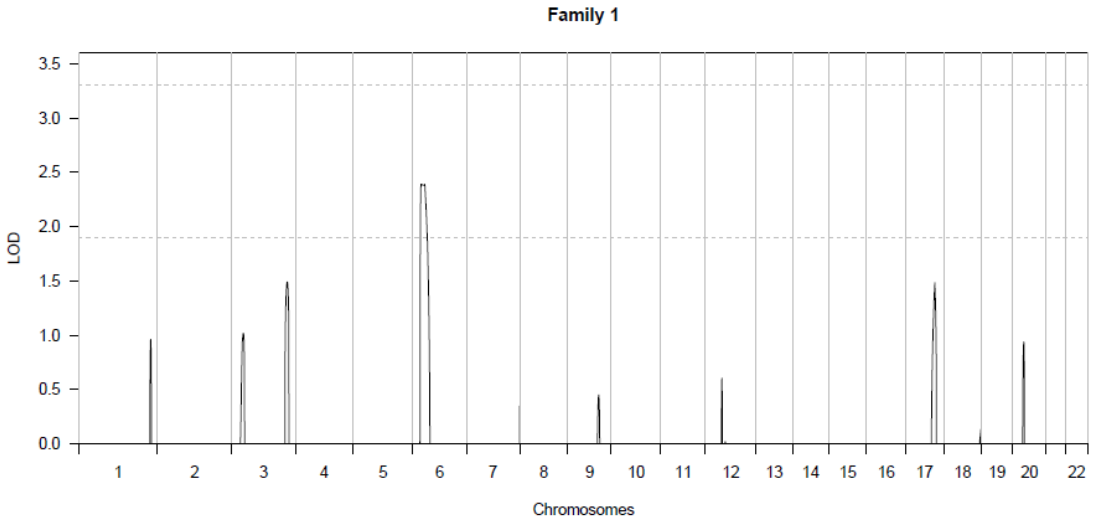
Family 1
LOD
3.5
3.0
2.5
2.0
1.5
1.0
0.5
0.0
1
2
3
4
5
6
7
8
9
10
11
12
13
14
15
16
17
18
19
20
22
Chromosomes

C

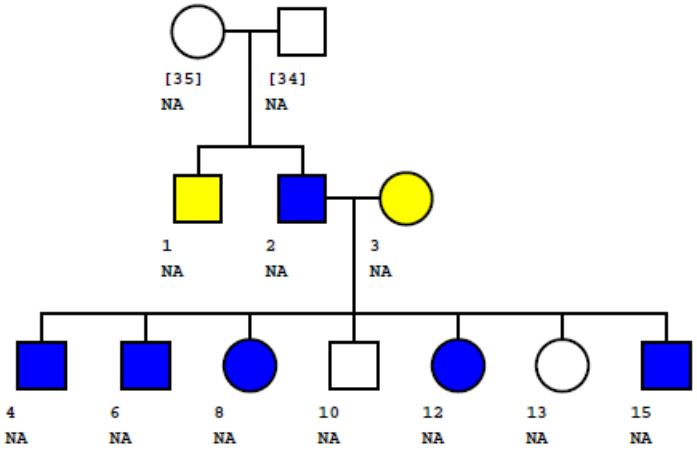

D

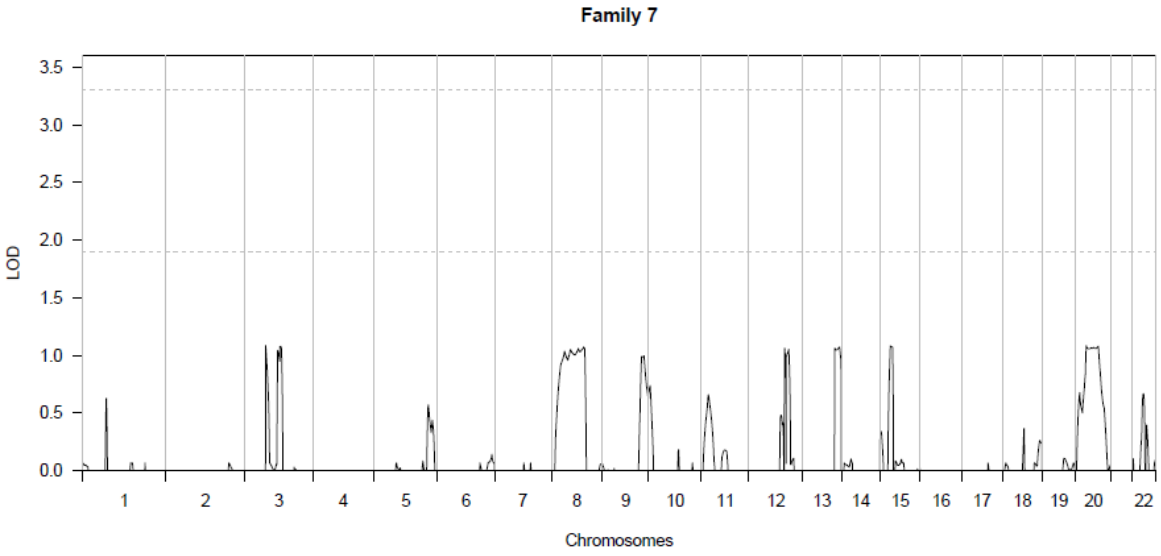

Supplementary Figure S3. Pedigrees and Linkage Analysis Results for Families #1 and #7. Panels A and C: Pedigrees for families 1 and 7, respectively. Affected males (squares) and females (circles) with carcinoid tumor appear as blue filled symbols. Subjects with unaffected and unknown disease status appear as yellow and empty symbols, respectively. Small Arabic numerals under a symbol identify individuals included in the linkage analysis (panels B and D) and brackets around these numerals indicate an individual for whom DNA was not available. NA indicates that the individual was included in the linkage analysis. Panels B and D: Results of a genome-wide multipoint linkage analysis for families #1 and #7 are shown in panels A and C, respectively. Shown are multi-marker LOD scores using a dominant inheritance model for all autosomes based on combined analysis of SNPs and microsatellites. Negative multipoint LOD scores are truncated at values of zero. LOD

score thresholds for suggestive (LOD ≥ 1.9) and genome-wide significance (LOD ≥ 3.3)[19] are shown as dotted lines. A suggestive linkage peak was observed for family 1 on chromosome 6 but this did not reach genome-wide significance and both families #7 and #9 showed negative multipoint LOD scores in this region of chromosome 6.

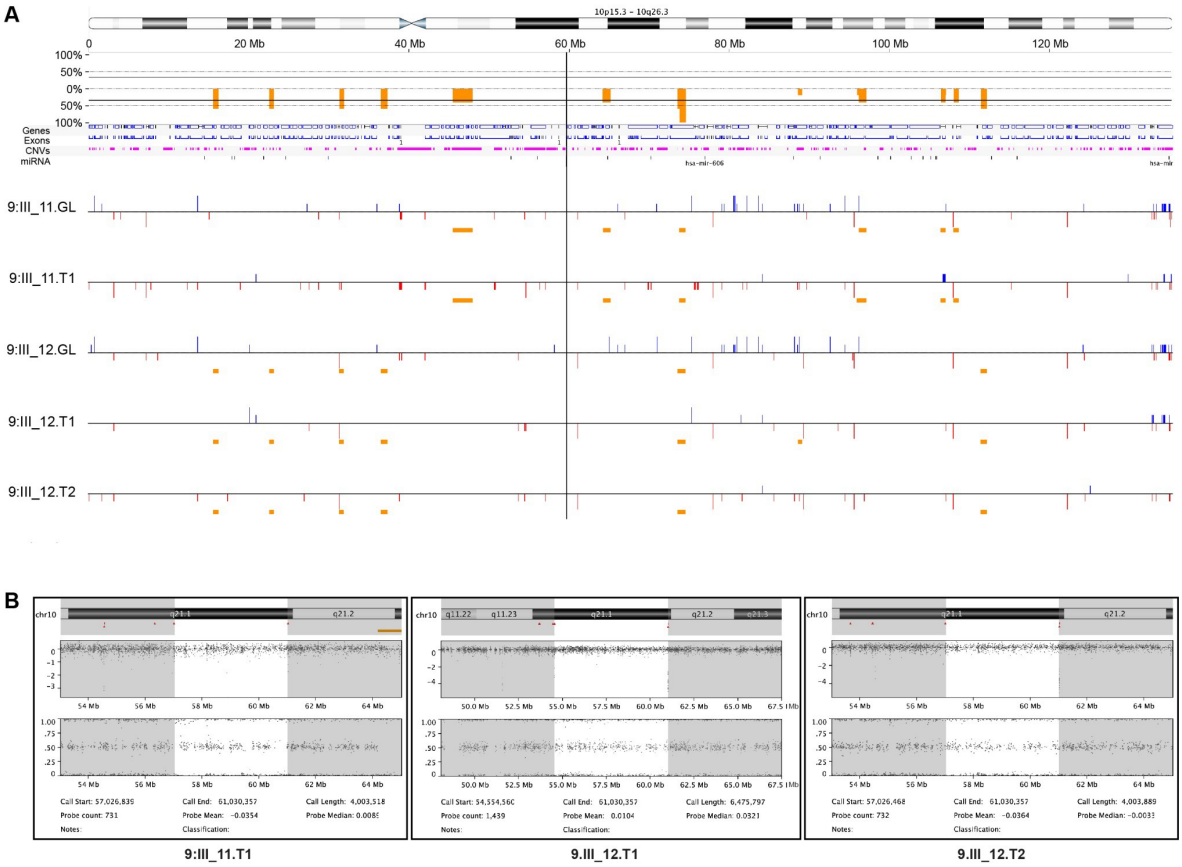

Supplementary Figure S4. Familial Carcinoid Tumor Analysis for Genomic Copy Number Variation (CNV). (A) Gross overview of the distribution of genomic CNV along chromosome 10 (idiogram at the top) for both germline((GL) and tumor (T) DNA for one tumor from subject 9:III_11 and two tumors from subject 9:III_12 using an Illumina 660W SNP array analyzed using Nexus 6.1 software (BioDiscovery Inc., Hawthorne, CA). Areas of DNA copy number gains (blue vertical lines, above horizontal), losses (red vertical lines, below horizontal) and losses of heterozygosity (LOH, orange below horizontal) are shown as vertical bars located along the sequence of chromosome 10. The gray vertical line crossing all analyses denotes the position of *IPMK* on chromosome 10. A summary analysis of CNV frequency for all of the samples is shown immediately below the chromosome 10 idiogram. Note that there are no areas of CNV, including LOH common to the tumors or even in any single tumor sample

relative to germline DNA in or around the position of *IPMK*. (B) High resolution view of the log R ratios (LRR, top) and B allele frequencies (BAF, bottom) for 731-1439 individual SNPS distributed along at least 4 million bp surrounding the position of *IPMK* for each of the tumors (9:III_11.T1, 9:III_12.T1 and 9:III_12.T2) . Note the absence of evidence for micro areas of CNV including LOH in and around *IPMK*.

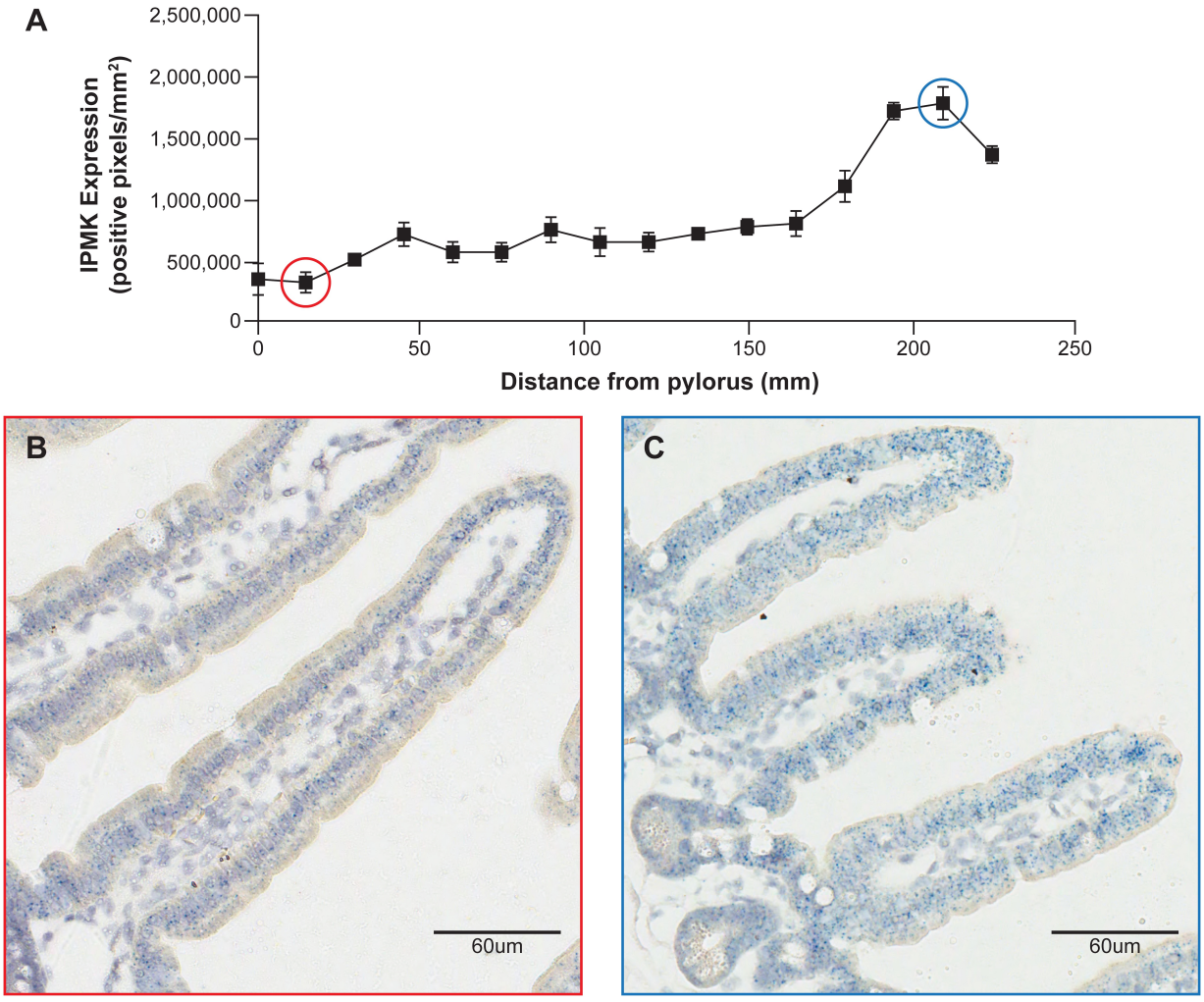

Supplementary Figure S5. Expression of *IPMK* transcripts in mouse small intestinal villi. (A) Quantitative analysis of *IPMK* RNA *in situ* hybridization (ISH) in FFPE mouse small intestinal villi. The distribution of *IPMK* expression along the small intestine was quantitated using image analysis software for chromogenic ISH (CISH) of mRNA probe signals (Fast blue dots, shown in panels B and C) in villi. Each data point was collected from scanned images of villi from 5 high powered fields (40X) sampled at 1.5 cm intervals and is expressed as the mean +/- SEM for positive blue pixels per mm^2 of villi. (B) and (C) Representative scanned images of duodenal and ileal villi taken at 1.5 (red circle) and 21 cm (blue circle) from the pylorus, respectively. Each blue dot represents a Fast blue signal from a single cRNA probe hybridized to an *IPMK* transcript.

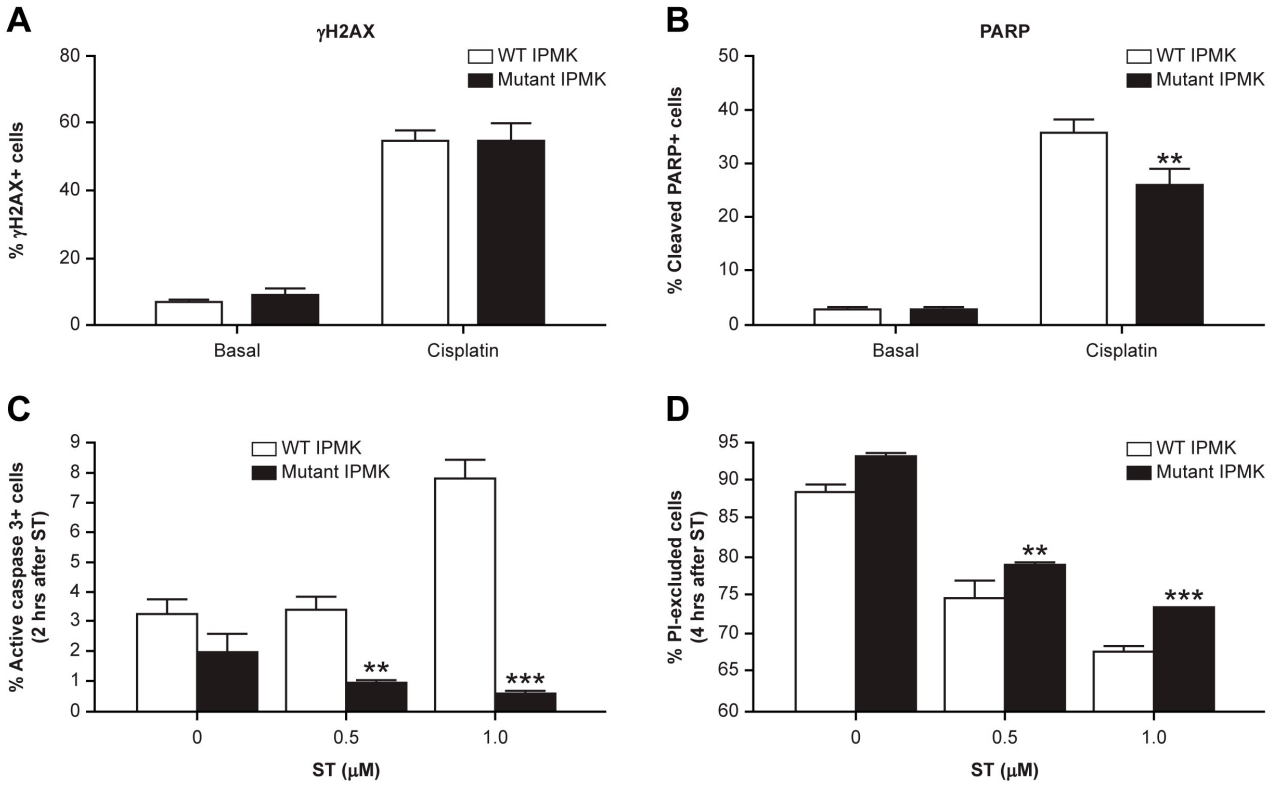

Supplementary Figure S6. Effect of IPMK Mutation on B lymphoblast Apoptotic Response to Genotoxic Stress. Panels A and B show the response of B lymphoblasts from carcinoid patients with the heterozygous 4 bp deletion mutation of IPMK to Cisplatin induced DNA damage and apoptosis, respectively, compared to normal control lymphoblasts. B lymphoblasts from IPMK mutant patients (n=4) and controls (n=7) were treated with and without cisplatin (50 uM) at 37^{o} C for 16 hrs. Levels of gH2AX and cleaved PARP were measured by indirect immunofluorescence and flow cytometry. Data show the mean +/-SEM, **p<0.01, Two-way ANOVA, Bonferroni post-hoc test. Panels C and D show the early apoptotic response of HEK293 cells expressing mutant IPMK versus WT IPMK. Twenty-four hours following transient transfection with either the 4 bp deletion mutant of IPMK or WT IPMK, HEK293 cells were treated with staurosporine, fixed, permeabilized, fluorescently labeled with FITC-conjugated anti-cleaved caspase-3 antibody and propidium iodide and analyzed using FACScan (BD Bioscience). Data show the mean +/- SEM, **p<0.01, ***p<0.001, two-way ANOVA.

A

920_921delAG	p.E307fs*31	337 a.a.	COSM1348355	Colon adenocarcinoma
986delA	p.H329fs*7	335 a.a.	COSM391624	Lung adenocarcinoma
990_993delCAGT	p.H330fs*4	333 a.a.	Novel	Small Intestinal-Carcinoid
956C>T	p.A319V	416 a.a.	COSM1492314	Kidney cancer
956C>G	p.A319G	416 a.a.	COSM1348354	Colon adenocarcinoma
965G>T	p.R322M	416 a.a.	COSM919140	Endometrial cancer
984G>C	p.K328N	416 a.a.	COSM1638601	Stomach adenocarcinoma

B

Supplementary Figure S7. Comparison of the Reported COSMIC IPMK Mutations located near the Truncation Mutation Reported Here for Small Intestinal Carcinoid Tumor. Panel A shows in tabular format the reported positions of the IPMK nucleotide deletion/s or missense mutations, the corresponding affected amino acid/s, affect on IPMK protein length, Catalogue of Somatic Mutations in Cancer (COSMIC) ID and associated affected organ, respectively. Panel B shows the location of the affected amino acid/s in the IPMK protein as a result of the nucleotide deletion/s or missense mutations corresponding to each of the designated affected tissues described in the table in panel A. NLS, nuclear localization signal sequence. Arabic numerals and arrows above the a.a. sequence denote the positions of the affected a.a. for the deletion mutations and the smaller font below the a.a. sequence denotes the a.a. substitutions for the missense mutations within this segment of the 416 a.a. IPMK protein sequence.

IV. Supplementary Tables

Supplemental Table S1. Clinical Data for Symptomatic Patients with Familial SI-NET.

	Pedigree #	Sex	Sx Age	Dx Age	Dx Delay	AAD	Survival yrs	Presenting Sxs	Stage	TNM	Grade	Tumor #/loc	Diagnostic Modality
1	1:II-1	F	62	71	9	72	1	P,D	IV	T4N1M1	G1	?/ileum	CT
2	1:II-2	M	59	60	1	78	18	N,V,F,O	IV	T4N1M1	NA		cholecystectomy
3	1:III-3	M	56	58	2	58	2	N,O,WL	IV	T4N1M1	G1	2/ileum	autopsy
4	2:II-1	M	64	64	0	68	4	P,D,F					barium swallow
5	2:III-1	M	29	52	23		L	F,B	IIIB	T3N1M0	G2	5/ileum	WCE/Octreo
6	2:III-2	M	25	45	20		L	P,F	IIIB	T3N1M0	G1	15/ileum	CT/CgA
7	3:II-1	M	54	56	2		L	B	IV	T4N1M1	G1	10/ileum	surg-SBO
8	3:II-7	F	47	54	7		L	P,O	IV	T4N1M1	G2	4/ileum	CT, MRI, US
9	4:II-1	F	50	77	27	87	10	F,O	IV	T4N1M1		multiple	exlap
10	4:III-3	F	66	67	1		L	O,WL	I	T1N0M0	G1	2/lung	CXR
11	4:III-4	M	68	68	1		L	P,B	IIIB	T4N1M0	G1	6/jej-ile	CT
12	5:II-1	M	45	45	0	45	<1	P,D,F,O	IV	T4N1M1	G1	1/ileum	CT
13	5:II-2	M	45	46	1	47	1	P,D,F,O	IV	T4N1M1	G1	1/ileum	CT/ Octr/Lbx
14	6:II-1	F	54	54	0		L	None	IIIB	T3N1M0		1/ileum	CT-(incidental)
15	6:II-2	F	44	52	8		L	P,F	IV	T4N1M1			CT/MRI/LBx
16	7:II-1	M	51	51	0	61	10	B	IIIB	T4N1M0	G1	12/ileum	WCE
17	7:III-7	M	40	60	20		L	P	IIIB	T4N1M0	G1	1/colon	exlap
18	8:II-1	F	63	63	0	78	15	O	IV	T4N1M1	G1	32/ileum	CT
19	8:III-1	F	44	45	1		L	None	IIIB	T2N1M0	G1	34/ileum	CT (incidental)
20	8:III-2	M	46	49	3		L	P,B	IV	T4N1M1	G1	27/ileum	WCE
21	9:II-1	M	65	70	5	70	<1	F,D	IV	T4N1M1	G2		exlap
22	9:II-2	F	80	87	7	87	<1	CHF,P					
23	9:II-3	M	83	83	0	86	3	P	IV	T4N1M1	G1	mult/SB	CT
24	9:II-4	M	63	77	14	77	<1	P	IV	T3N1M1	G1	>5/SB	
25	9:II-5	F	63	65	2	67	2	P	IV	T4N1M1			exlap
26	9:III-9	F	56	56	0	58	2	O	IV	T4N1M1	G1	4	
27	9:III-25	M	NA	33	NA		L	None				1/lung	chest CT
28	10:II-1	F	67	67	NA	74	7	F	IV	T4N1M1	G1	mult/ileu	US (incidental)
29	10:II-2	M	42	43	1	60	17	F,D	IV	T4N1M1			CT/chem/Lbx
30	11:II-1	M	72	78	6	88	10	O	IV	T4N1M1	G1	1/ileum	exlap
31	11:II-2	F	70	79	9		L	F,D					exlap
32	12:II-1	F	58	61	NA	61	<1	F,P	IV	T4N1M1			Autopsy
33	12:III-1	M	65	67	2		L	F,D	IV	T4N1M1	G1	10/ileum	CT/US/Lbx
34	12:IV-4	F	44	44	0		L	P	I	T1N0M0	G1	1/append	exlap/appy
35	13:II-1	F	45	64	9		L	P,D,O	IV	T4N1M1	G2	1/ileum	CT/MRI/Lbx
36	13:II-2	M	58	59	1		L	P	IV	T4N1M1		1	
37	13:III-2	M	51	51	<1		L	P	IV	T4N1M1	G1	9	CT
38	14:II-1	M	74	74	<1	82	8	F,D,P,WL	IV	T4N1M1		1	CT/Octreo
39	14:II-2	M	43	61	18	65	4	P,D,F,O	IV	T4N1M1			exlap
40	15:II-1	M		56		58	2	F,D	IV	T4N1M1	G1	NA	Lbx
41	15:II-2	M	55	58	3		L	D,B	IV	T4N1M1	G1	50/ileum	CT/exlap
42	16:II-2	M	51	51	0		L	P	IIIB	T3N1M0	G1	2/ileum	CT
43	16:III-1	F	16	22	4		L	P	IIA	T2N0M0	1	1/append	exlap/Appy
44	17:II-1	F	61	62	1	88	16	P	I	TxN0M0			
45	17:III-1	M	63	63	0		L	B, CHF	IV	T4N1M1	G1	1/ileum	CT/Octr/US
46	17:III-2	F	50	60	10		L	F,D,P	IV	T4N1M1	G1	9/jejunum	CT/Octr
47	18:II-1	M	53	63	10	67	4	P,D	IV				exlap/5-HIAA
48	18:III-1	F	55	69	14		L	P	IV	T4N1M1	G1	4/ileum	CT
49	19:I-1	F	66	69	3	76	7	P,O	IIA	T2N0M0			exlap
50	19:II-1	F	49	50	1	57	7	D	IV	T4N1M1			WCE/exlap
51	20:II-1	F	55	84	29	87	3	O	IV	T4N1M1	G1	1/ileum	FNA-LN
52	20:III-1	F	51	53	2		L	P	IIIB	T4N1M0	G1	1/jejunum	CT
53	21:II-1	F	55	71	16	83	12	P,D	IV	T4N1M1	G1	3/SB	CT/serotonin
54	21:III-1	F	55	57	2		L	F	IV	T4N1M1	G1	mult/ileu	CT
55	22:II-1	M	83	83	0		L	P,F,D	IV	T4N1M1	G1	2/ileum	CT
56	22:III-1	F	46	46	0		L	B	IIIB	T4N1M0	G1	2/ileum	WCE
57	23:II-1	F	57	59	2		L	P	IV	T4N1M1	G1	25/ jej-ile	CT

58	23:II-2	M	61	61	0	64	3	P	IV	T4N1M1			CT/exlap
59	24:II-1	M	81	81	1	83	2	P, B, DBM	IIIB	T4N1M0	G1	1/ileum	colonoscopy
60	24:III-1	M	66	67	1		L	F,P	IV	T4N1M1			CT/5-HIAA
61	25:II-1	M	83	85	2	85	<1	Constip	IIIA		G1	7/ileum	exlap
62	25:III-1	F	54	56	2		L	P	IV	T4N1M1			ascitic cytology
63	26:II-2	F				67	D		IV				
64	26:II-3	F	77	77	0	78	1	PO	IV		G1		ascites exlap
65	27:II-1	M		82		83	1	P,WL,D	IV	T4N1M1		1/ileum	exlap
66	27:III-1	F	69	71	2		L	P	IIIB	T3N1M0	G1		chole (incidental)
67	28:II-1	M	70	71	1	71	<1	P,O	IV	T4N1M1	G2	?/jejunum	exlap
68	28:III-3	M	45	45	0		L	P,O	IIIB	T3N1M0	G1	11/jej-ile	exlap
69	29:I-1	F	69	69	0		L	P	IIIB	T3N1M0	G1	2/ileum	CT
70	29:II-1	F	23	27	4		L	P,D,F	IV	T4N0M1	G1	2/ileum	CT/serotonin
71	30:II-1	M	44	50	6	65	15	P,D	IIIB	T4N1M0	G1	1/ileum	exlap
72	30:III-1	F	44	50	6		L	P	IV	T4N1M1	G1	5/ileum	CT/exlap
73	31:II-1	F	62	64	2		L	P,N,V,C	IV	T4N1M1	G1	4/ileum	MRI
74	31:II-2	F	49	59	10		L	P,N,V,O	IIIB	T3N1M0	G1	2/ileum	exlap
75	32:III-1	F	47	49	2		L	P	IV	T4N1M1	G1	7/ileum	chole (incidental)
76	33:I-1	F	65	65	0	79	14	P,N,V	IIIB	T4N1M0	G1	2/ileum	abd-xray
77	33:II-1	F	61	65	4		L	P,D,F	IV	T4N1M1	G1	1/ileum	CT

Notes: M, Male; F, Female; Pedigree # denotes the family #, Roman numeral the generation and Arabic # the position within a generation (Supplementary figure S1); Sx Age, age when first symptomatic; Dx Age, age at diagnosis; Dx Delay, diagnostic age minus symptomatic age; AAD, age at death; Survival, AAD minus Dx Age; L, living; D, dead, unknown interval since diagnosis; Presenting sxs: B, GI bleeding; C, constipation; D, diarrhea; F, flushing; P, abdominal pain; WL, weight loss; Bowel Tumors, # found at surgery; Lymph Nodes, # positive for tumor at pathology. TNM Class, classification used for staging based upon tumor size and invasion depth, lymph node metastases and distant metastases. NA, not applicable; Grade, based upon mitotic index and Ki-67. Tumor #/location, number of tumors found in that segment of bowel; mult, multiple; SB, small bowel (when segment not specified in medical record); ?, # of tumors not reported in medical record. Diagnostic Modality: Exlap, exploratory laparotomy; Appy, appendectomy; WCE, wireless capsule endoscopy; Octreo, Octreoscan; CT, computerized tomography; FNA-LN, fine needle aspiration of a lymph node; US, abdominal ultrasound; MRI, magnetic resonance imaging; Chole, cholecystectomy; Incidental, unintended finding; 5-HIAA, 5-hydroxy indoleacetic acid; Lbx, liver biopsy.

Supplementary Table S2. Clinical Data for Asymptomatic Patients Who Screened Positive for Familial SI-NET.

	Pedigree #	Age	Sex	Diagnostic Modality	Bowel Tumors (#)	Lymph Nodes (#)	Primary Size (mm)	TNM Class	Stage	Grade	Site, LO R (cm)	DOS	NED (months)
1	1:III-1	53	F	CT, PET, WCE	4	7	16	T1N1M0	IIIB	G1	J-I, 100	09/14/09	61
2	1:III-2	55	M	PET,WCE	11	0	5	T1N0M0	I	G1	I, 110	10/28/09	59
3	1:III-7	61	F	PET,WCE	4	2	2	T4N1M0	IIIB	G1	J-I, 100	12/14/09	58
4	1:III-8	56	F	CT, PET, WCE	8	3	10	T4N1M0	IIIB	G1	J-I, 90	09/14/09	61*
5	3:II-5	62	M	CT, WCE, MRI	9	6	12	T2N1M0	IIIB	G1	I, 77	08/03/11	38
6	4:III-2	71	F	PET/CT, WCE	1	0	8	T1N0M0	I	G1	I, 42	01/16/13	20
7	7:III-1	44	F	PET, WCE	1	0	2	T1N0M0	I	G1	J, 55	01/05/11	44
8	7:III-2	45	F	CT, PET, WCE	3	0	8	T3N0M0	IIB	G1	I, 130	03/10/09	67
9	7:III-4	48	M	WCE	2	0	1	T1N0M0	I	G1	J, 90	03/30/09	66
10	7:III-6	51	M	CT, PET, WCE, 5-HIAA	6	11	21	T4N1M1	IV	G1	J-I, 150	05/11/09	NA
11	9:III-2	67	F	WCE	1	0	5	T1N0M0	I	G1	J, 20	01/15/09	68
12	9:III-11	65	M	CT, PET, WCE	2	0	6	T1N0M0	I	G1	J-I, 75	02/01/10	56
13	9:III-12	60	M	CT, WCE	5	0	5	T2N0M0	IIA	G1	I, 45	03/04/09	67
14	9:III-15	60	M	5-HIAA	NA	NA	NA	NA	NA	NA	NA	NA	NA
15	9:III-17	56	M	CT	NA	NA	NA	NA	NA	NA	NA	NA	NA
16	9:III-22	57	M	PET, WCE	7	1	7	T4N1M0	IIIB	G1	J, 75	01/15/09	68
17	10:II-3	56	M	CT, PET, WCE	3	0	6	T1N0M0	I	G1	I, 81	02/24/10	55
18	10:III-3	52	F	CT, PET, WCE	10	15	25	T4N1M0	IIIB	G2	I, 70	06/14/10	52
19	14:III-1	56	M	WCE	4	0	8	T1N0M0	I	G1	I, 75	07/12/11	38
20	18:III-2	74	M	CT, PET, WCE	9	3	11	T3N1M1	IV	G1	J, 85	10/31/11	NA
21	22:II-2	68	M	PET/CT	1	0	8	T2N0M0	IIA	G1	I, 7.5	09/12/12	25
22	26:II-1	79	M	PET/CT	NA	NA	NA	NA	NA	NA	NA	NA	NA
23	26:III-2	58	M	CT, PET/CT, WCE	29	4	11	T2N1M0	IIIB	G1	I, 195	03/02/12	31
24	26:III-4	62	F	CT,PET/CT,WCE	9	1	5	T2N1M0	IIIB	G1	I, 42	06/14/12	28
25	26:III-5	63	F	WCE	1	0	4	T2N0M0	IIA	G1	I, 16.5	09/17/12	25
26	29:III-2	43	F	CT,PET/CT,WCE	2	0	9	T2N0M0	IIA	G1	J, 25	10/17/12	24

Notes: Age, age at time of diagnosis; M, Male; F, Female; Pedigree #, family: generation-position within generation (Supplementary figure S1); Diagnostic Modality, CT (computerized tomography), PET (positron emission tomography), WCE (wireless capsule endoscopy), 5-HIAA (5-hydroxyindoleacetic acid); Bowel Tumors (#), # found at surgery; Primary Size (mm), size of largest primary tumor; Lymph Nodes, # positive for tumor at pathology. TNM Class, classification used for staging based upon tumor size and invasion depth, lymph node metastases and distant metastases. NA, not applicable; Grade, based upon mitotic index and Ki-67. Site, LOR, SI segment with tumor and length of bowel resection; DOS, date of surgery

in MM/DD/YY format. NED, duration of No Evidence of Disease relative to DOS. * denotes no new tumor beyond a residual unresected single mesenteric lymph node.

Supplementary Table S3. Sanger Sequencing Verification of Shared Mutations Identified from Whole Exome Sequencing of Germline DNA.

	Gene	Chr	CDS	Chr Position	Reference	Mutation	AA Change	9:II-3	9:III-2	9:III-9	9:III-11	9:III-12	9:III-22
1	USP17L1 0	4	1	9213672	G	1290G>C	430Q>H	Yes	ND	ND	No	Yes	Yes
2	USP17L1 1	4	1	9217197	T	64T>C	23S>P	Yes	ND	ND	No	Yes	Yes
3	IPMK	10	6	59956092	C	delCTGA	FS	Yes	Yes	Yes	Yes	Yes	Yes
4	IPMK	10	6	59956093	T	-	-	Yes	Yes	Yes	Yes	Yes	Yes
5	IPMK	10	6	59956094	G	-	-	Yes	Yes	Yes	Yes	Yes	Yes
6	IPMK	10	6	59956095	A	-	-	Yes	Yes	Yes	Yes	Yes	Yes
7	KRTAP4- 8	17	1	39254336	T	insT	FS	Yes	ND	ND	No	Yes	No

Notes: Listed gene mutations were shared among the five affected members of family 9 (9:II-3, 9:III-2, 9:III-11, 9:III-12 and 9:III-22, Fig. 2A) following WES and variant analysis filtering as described in the methods section, Whole Exome Sequencing (WES) and Variant Analysis. These gene mutations were target sequenced by Sanger's method using germline DNA from four (9:II-2, 9:III-15, 9:III-17, 9:III-25, Fig 2A) of the six affected family members not analyzed by WES. The two remaining affected members (9:II-5 and 9:III-9, Fig. 2A) for whom only archival DNA was available, were sequenced for verification of the *IPMK* mutation only. ND, not done.

V. Supplementary References

1. Matise TC, Chen F, Chen W, et al. A second---generation combined linkage physical map of the human genome. Genome Res 2007;17:1783---6.
2. **Van Loo P, Nordgard SH**, Lingjærde OC, et al. Allele---specific copy number analysis of tumors. Proc Natl Acad Sci U S A 2010;107:16910---5.
3. Olshen AB, Venkatraman ES, Lucito R, et al. Circular binary segmentation for the analysis of array---based DNA copy number data. Biostatistics 2004;5:557---72.
4. Sobel E, Lange K. Descent graphs in pedigree analysis: applications to haplotyping, location scores, and marker---sharing statistics. Am J Hum Genet 1996;58:1323---37.
5. Cottingham RW, Jr., Idury RM, Schäffer AA. Faster sequential genetic linkage computations. Am J Hum Genet 1993;53:252---63.
6. Schäffer AA, Gupta SK, Shriram K, et al. Avoiding recomputation in linkage analysis. Hum Hered 1994;44:225---37.
7. Ott J. Computer---simulation methods in human linkage analysis. Proc Natl Acad Sci U S A 1989;86:4175---8.
8. Schäffer AA, Lemire M, Ott J, et al. Coordinated conditional simulation with SLINK and SUP of many markers linked or associated to a trait in large pedigrees. Hum Hered 2011;71:126---34.
9. Ge D, Ruzzo EK, Shianna KV, et al. SVA: software for annotating and visualizing sequenced human genomes. Bioinformatics 2011;27:1998---2000.
10. Girish V, Vijayalakshmi A. Affordable image analysis using NIH Image/ImageJ. Indian J Cancer 2004;41:47.
11. **Maag D, Maxwell MJ**, Hardesty DA, et al. Inositol polyphosphate multikinase is a physiologic PI3--- kinase that activates Akt/PKB. Proc Natl Acad Sci U S A 2011;108:1391---6.
12. Koldobskiy MA, Chakraborty A, Werner JK, Jr., et al. p53---mediated apoptosis requires inositol hexakisphosphate kinase---2. Proc Natl Acad Sci U S A 2010;107:20947---51.
13. Morrison BH, Haney R, Lamarre E, et al. Gene deletion of inositol hexakisphosphate kinase 2 predisposes to aerodigestive tract carcinoma. Oncogene 2009;28:2383---92.
14. Maffucci T, Piccolo E, Cumashi A, et al. Inhibition of the phosphatidylinositol 3---kinase/Akt pathway by inositol pentakisphosphate results in antiangiogenic and antitumor effects. Cancer Res 2005;65:8339---49.
15. Piccolo E, Vignati S, Maffucci T, et al. Inositol pentakisphosphate promotes apoptosis through the PI 3---K/Akt pathway. Oncogene 2004;23:1754---65.
16. Gao Y, Wang H-Y. Inositol pentakisphosphate mediates Wnt/beta---catenin signaling. J Biol Chem 2007;282:26490---502.
17. Wang Y, Wang H-Y. Dvl3 translocates IPMK to the cell membrane in response to Wnt. Cell Signal 2012;24:2389---95.
18. **Wickramasinghe VO, Savill JM**, Chavali S, et al. Human inositol polyphosphate multikinase regulates transcript---selective nuclear mRNA export to preserve genome integrity. Mol Cell 2013;51:737---50.
19. Lander E, Kruglyak L. Genetic dissection of complex traits: guidelines for interpreting and reporting linkage results. Nat Genet. 1995;11(3):241---7.

Author names in bold designate shared co-first authors.